

## Prediction of ultimate shear strength and failure modes of R/C ledge beams using machine learning framework

Ahmed M. Yousef<sup>1</sup>, Karim Abd El-Hady\*<sup>2</sup> and Mohamed E. El-Madawy<sup>1</sup>

<sup>1</sup>Department of Structural Engineering, Faculty of Engineering, Mansoura University, El-Mansoura, 35516, Egypt

<sup>2</sup>Department of Civil Engineering, Faculty of Engineering, Damietta University, New Damietta, 34517, Egypt

(Received May 31, 2022, Revised December 10, 2022, Accepted December 12, 2022)

**Abstract.** The objective of this study is to present a data-driven machine learning (ML) framework for predicting ultimate shear strength and failure modes of reinforced concrete ledge beams. Experimental tests were collected on these beams with different loading, geometric and material properties. The database was analyzed using different ML algorithms including decision trees, discriminant analysis, support vector machine, logistic regression, nearest neighbors, naïve bayes, ensemble and artificial neural networks to identify the governing and critical parameters of reinforced concrete ledge beams. The results showed that ML framework can effectively identify the failure mode of these beams either web shear failure, flexural failure or ledge failure. ML framework can also derive equations for predicting the ultimate shear strength for each failure mode. A comparison of the ultimate shear strength of ledge failure was conducted between the experimental results and the results from the proposed equations and the design equations used by international codes. These comparisons indicated that the proposed ML equations predict the ultimate shear strength of reinforced concrete ledge beams better than the design equations of AASHTO LRFD-2020 or PCI-2020.

**Keywords:** algorithms; failure modes; ledge beams; machine learning framework; reinforced concrete; ultimate shear strength

### 1. Introduction

Reinforced concrete inverted-T bent caps (beams with ledges) are being used as the main girders that support the lateral, secondary and incoming beams or slabs which is one of the common structural systems for many existing bridges and parking garages. Reinforced concrete ledge beams are often used in construction to decrease the overall height of bridges and to improve available clearance below the beams. The use of reinforced concrete ledge beams can result in large savings in the overall cost of the bridge and lead to more appealing bridges. In buildings, the use of reinforced concrete ledge beams decrease for the overall story heights (Mirza *et al.* 1983, Deifalla and Ghobarah 2014, Varney *et al.* 2015, Garber *et al.* 2017).

The behavior of reinforced concrete ledge beams, despite its usual use since the 1950s, continued to be as one of the least investigated until mid-1980s. Until that time, no instruction for handling design issues specifically those related to the inverted-T section was available in design standards.

---

\*Corresponding author, MSc. Student, E-mail: karimabdelhady@du.edu.eg

One of the main complications to the design of these beams is the behavior of the ledge. The cross-section shape can have a considerable effect on the behavior and design, as concluded by several researchers (Furlong and Ferguson 1971, Mirza and Furlong 1985, Chalioris and Karayannis 2009, Deifalla and Ghobarah 2006a, b, Karayannis 1995, Karayannis and Chalioris 2000). Many experimental studies were made on reinforced concrete ledge beams with various cross sections and loading characteristics. These studies aim to know the structural behavior and the response of reinforced concrete ledge beams (Smith and Fereig 1977, Tan *et al.* 1997, Zhu *et al.* 2003, Fernandez Gomez 2012, Larson *et al.* 2013, Garber *et al.* 2017, Galal and Sekar 2008, Salman *et al.* 2019, Hedia *et al.* 2020).

Recently, design provisions for predicting the ultimate shear strength and failure modes of reinforced concrete ledge beams have been developed and incorporated in some codes. In the united states, the American Association of State High ways Transportation Officials (AASHTO LRFD-2020) [29], the Strut and Tie Method (STM) with regard to the American Concrete Institute Code (ACI 318-2019) and the design handbook of Prestressed Concrete Institute (PCI-2020) include provisions for predicting the ultimate strength and failure modes of reinforced concrete ledge beams.

Machine learning (ML) is a branch of artificial intelligence that uses algorithms to develop patterns in data and make predictions about the future. The success of ML applications in areas such as bioengineering, medicine, and advertising has been highly obvious (Cheung *et al.* 2008, Gui *et al.* 2017, Gul and Catbas 2009, Salehi *et al.* 2018, 2019). In the last decade the community of structural engineering researchers have begun to seriously search for ways in which ML can improve the efficiency and accuracy of specific tasks or solve previously complex problems. Machine learning framework is being used recently in many structural engineering applications such as structural system identification, structural health monitoring, structural vibration control, structural design and prediction applications (Chou *et al.* 2014, Dantas *et al.* 2013, González and Zapico 2008, Reddy *et al.* 2011, Siddique and Aggarwal 2011, Yan and Shi 2010). ML framework is essential in prediction of properties of concrete beams (Solhmirzaei *et al.* 2020, Markou and Bakas 2021, Rahman *et al.* 2021, Zhang *et al.* 2020, Ly *et al.* 2020, Abuodeh *et al.* 2020, Wakjira *et al.* 2022, He *et al.* 2022, Uddin *et al.* 2022).

The behavior of the ledges is one of the main issues that arise when designing ledge beams. Although they have a better profile, the complicated load transfer mechanism makes designing beams with ledges difficult. In comparison to conventional rectangular or T beams, the behavior of inverted-T beams is more complex. For instance, the ledge is subjected to loads from bridge girders that flow transversely to the web's bottom, vertically to the top compression chord, and finally along the beam's length to the supports on either end. In order to facilitate the design of these beams, it is very important to develop a ML framework to predict the ultimate shear strength and failure mode of RC ledge beams and improve the use of these beams in concrete structures

The aim of this study is to propose expressions to predict ultimate shear strength and failure modes of reinforced concrete ledge beams using ML framework based on collected experimental data. In addition, a comparison was conducted between ultimate shear strength of ledge failure predicted from the proposed equations and that from the experimental results and that from the design equations of AASHTO LRFD-2020 and PCI-2020.

## 2. Types of failures in reinforced concrete ledge beams

In the design of reinforced concrete ledge beam or any other ledged members, the following three

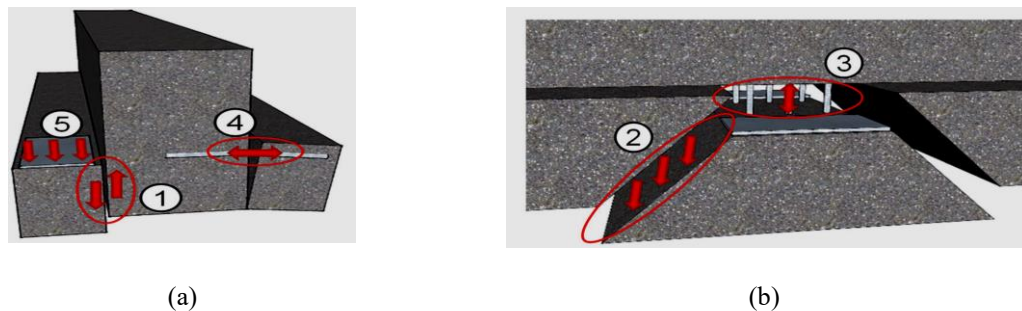


Fig. 1 (a) Cross section and (b) longitudinal section with typical types of ledge failures: 1) shear friction; 2) punching shear 3) yielding of hanger reinforcement; 4) flexural failure of ledge and 5) bearing failure

main types of failures must be considered:

- i. Web shear failure.
- ii. Flexural failure.
- iii. Ledge failure as shown in Fig. 1, and it can be divided into the following types:
  - Shear friction failure between the ledge and the web.
  - Punching shear failure of the ledge at the point of loading.
  - Yielding of hanger reinforcement.
  - Flexural failure of ledge reinforcement.
  - Bearing failure of concrete under the load point.

## 2. Database collection

A literature review was done to collect data from experiments conducted on Normal Strength Concrete (NSC) and High Strength Concrete (HSC) ledge beams. Many parameters affect the behavior of reinforced concrete ledge beams such as type and strength of concrete, web dimensions, ledge dimensions, web reinforcement ratio, ledge reinforcement ratio, shear span to depth ratio and load points. These parameters are used to predict ultimate shear strength and failure modes of reinforced concrete ledge beams.

A total of 130 specimens from different sources were included and filtered in the collection database (Fernandez Gomez 2012, Larson *et al.* 2013, Garber *et al.* 2017, Galal and Sekar 2008, Salman *et al.* 2019, Hedia *et al.* 2020). Twenty seven specimens tested under torsional loads couldn't be used. In addition, forty nine specimens have not sufficient information to make data base. Table 1 provides the filtered database as it was reduced to 54 tests that have detailed information to perform various analyses and build a comprehensive database.

The database contains a summary of selected experimental specimens with design variables including  $f'_c$  (Compressive strength of concrete),  $f_{cu}$  (Cube compressive strength of concrete),  $d$  (Beam depth),  $b$  (Beam width),  $b_w$  (Beam web width),  $L_d$  (Ledge depth),  $L_w$  (Ledge width),  $L_l$  (Ledge length),  $a/d$  (Shear span-to-depth ratio with shear span measured from center of reaction to the first reaction point),  $\rho_v$  (Web vertical reinforcement ratio),  $f_{yv}$  (Yield strength of web vertical reinforcement),  $\rho_h$  (web horizontal reinforcement ratio),  $f_{yh}$  (Yield strength of web horizontal reinforcement),  $\rho_l$  (Vertical reinforcement ratio of ledge),  $f_{yl}$  (Yield strength of vertical

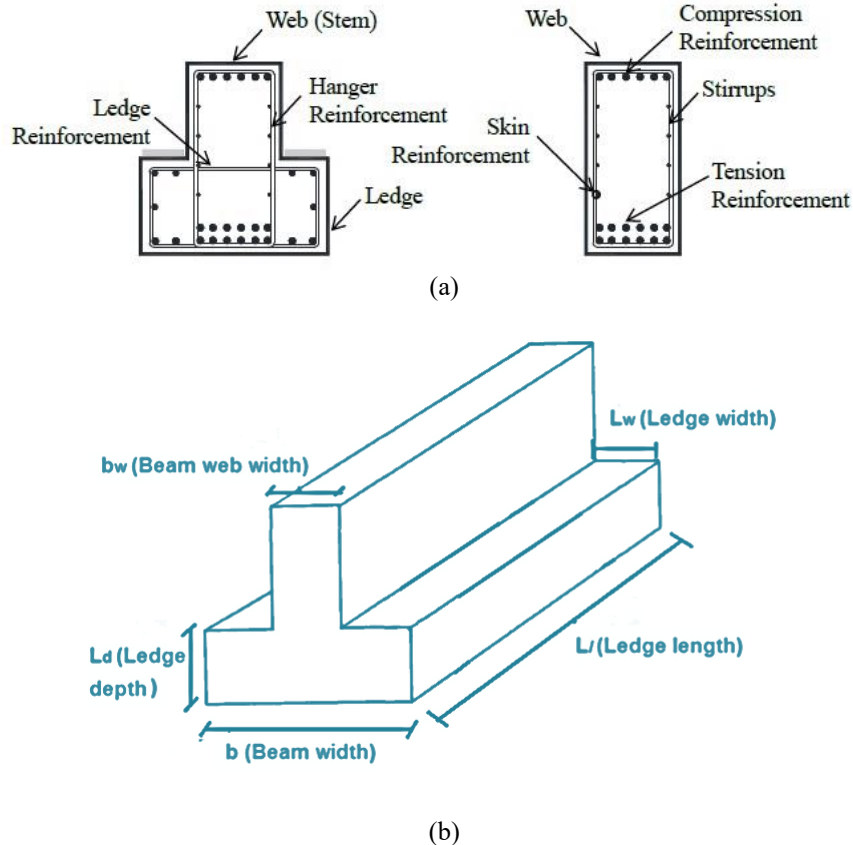


Fig. 2 (a) Typical reinforcement details of ledge beams and (b) Different design variables for reinforced concrete ledge beams

reinforcement of ledge) and  $V_u$  (Ultimate shear carried in the critical section of the test region). The design variables and reinforcement details for reinforced concrete ledge beams can be seen from Fig. 2. The number of times that each value or range of the variables appear in the database is shown in Fig. 3.

#### 4. ML Framework for prediction of failure mode

##### 4.1 General

ML trains models to classify data by using the best classification model type including decision trees, discriminant analysis, support vector machines, logistic regression, nearest neighbors, naive bayes, ensemble and neural network classification. In this study, ML framework implemented in the programming system and language MATLAB 2020 (Yang *et al.* 2020) was applied for the collected experimental data in order to train the best model that generates predictions for the failure mode as shown in Fig. 4.

Table 1 Collected specimens for reinforced concrete ledge beams from tests

Ref	Specimen ID	Concrete	$f'_c$ (MPa)	b (mm)	$b_w$ (mm)	$L_d$ (mm)	$L_w$ (mm)	$L_l$ (mm)	a/d	$\rho_v$ (%)	$f_{yv}$ (MPa)	$\rho_h$ (%)	$f_{yh}$ (MPa)	$\rho_l$ (%)	$f_{yl}$ (MPa)	$v_u$ (KN)	Failure Mode
	DS1-42-1.85-03	NSC	36.3	1067	533	533	267	3845	1.96	0.30	434	0.30	434	0.19	434	3167	Web Shear
	DS1-42-2.50-03	NSC	37.2	1067	533	533	267	3845	2.65	0.30	434	0.30	434	0.19	434	1806	Web Shear
	DS1-42-1.85-06	NSC	34.6	1067	533	533	267	4093	1.85	0.60	421	0.60	421	0.19	421	2762	Web Shear
	DS1-42-2.50-06	NSC	35.1	1067	533	533	267	4093	2.5	0.60	421	0.60	421	0.19	421	2237	Web Shear
	DL1-42-1.85-06	NSC	33.3	1067	533	533	267	6482	1.85	0.60	421	0.60	421	0.19	421	3296	Web Shear
	DL1-42-2.50-06	NSC	34.4	1067	533	533	267	6482	2.5	0.60	421	0.60	421	0.19	421	2767	Web Shear
	SS3-42-1.85-03	NSC	40.6	1067	533	356	267	4093	1.85	0.30	462	0.30	462	0.28	462	2326	Web Shear
	SS3-42-2.50-03	NSC	40.6	1067	533	356	267	4093	2.5	0.30	462	0.30	462	0.28	462	1988	Web Shear
	SS3-42-2.50-06	NSC	43.2	1067	533	356	267	3434	2.5	0.60	421	0.60	421	0.28	421	2295	Flexural
	SC3-42-2.50-03	NSC	40.5	1067	533	356	267	2479	2.5	0.30	441	0.30	441	0.28	441	1463	Web Shear
	SC3-42-1.85-03	NSC	40.5	1067	533	356	267	2479	1.85	0.30	441	0.30	441	0.28	441	2148	Web Shear
	DS3-42-2.50-03	NSC	39.2	1067	533	533	267	3434	2.5	0.30	448	0.30	448	0.19	448	1913	Web Shear
	DL1-42-1.85-03	NSC	34	1067	533	533	267	6482	1.85	0.30	441	0.30	441	0.19	441	2785	Web Shear
	DL1-42-2.50-03	NSC	34	1067	533	533	267	6482	2.5	0.30	441	0.30	441	0.19	441	2269	Web Shear
	SL3-42-1.85-03	NSC	34.7	1067	533	356	267	6482	1.85	0.30	455	0.30	455	0.28	455	2540	Web Shear
	SL3-42-1.85-06	NSC	36.2	1067	533	533	267	6482	1.85	0.60	448	0.60	448	0.19	448	3309	Web Shear
(Fernandez Gomez 2012, Larson et al. 2013)	DC1-42-1.85-06	NSC	25.7	1067	533	533	267	3100	1.85	0.60	421	0.60	421	0.19	421	2309	Web Shear
	SS1-75-1.85-03	NSC	21.6	1067	533	635	267	3845	1.87	0.30	448	0.30	448	0.15	448	3314	Web Shear
	DC3-42-1.85-03	NSC	31.5	1067	533	533	267	3100	1.85	0.30	434	0.30	434	0.28	434	1757	Web Shear
	DS3-42-1.85-03	NSC	31.5	1067	533	533	267	4752	1.85	0.30	434	0.30	434	0.28	434	2019	Web Shear
	SS1-42-2.50-03	NSC	39.3	1067	533	356	267	4093	2.5	0.30	462	0.30	462	0.19	462	1770	Web Shear
	SS1-42-1.85-03	NSC	39.4	1067	533	356	267	4093	1.85	0.30	462	0.30	462	0.19	462	2593	Web Shear
	DC1-42-2.50-03	NSC	27.8	1067	533	533	267	2479	2.5	0.30	427	0.30	427	0.28	427	1624	Web Shear
	DL3-42-1.85-03	NSC	29	1067	533	533	267	6482	1.85	0.30	427	0.30	427	0.28	427	2798	Flexural
	SL1-42-2.50-03	NSC	29.5	1067	533	356	267	6482	2.5	0.30	441	0.30	441	0.19	441	2215	Web Shear
	SC1-42-2.50-03	NSC	29.5	1067	533	356	267	2479	2.5	0.30	441	0.30	441	0.19	441	1419	Ledge (Shear friction)
	DS1-42-1.85-06/03	NSC	28.8	1067	533	533	267	4093	1.85	0.60	448	0.30	448	0.28	448	2398	Web Shear
	DS1-42-2.50-06/03	NSC	28.8	1067	533	533	267	4093	2.5	0.60	448	0.30	448	0.28	448	3287	Web Shear
	SC1-42-1.85-03	NSC	29.9	1067	533	356	267	2479	1.85	0.30	462	0.30	462	0.19	462	2060	Ledge (Yield of ledge tie)
	DC1-42-1.85-03	NSC	29.6	1067	533	533	267	2479	1.85	0.30	462	0.30	462	0.28	462	3000	Web Shear
	SC1-42-1.85-03	NSC	20.8	1067	533	356	267	2479	1.85	0.30	476	0.30	476	0.19	476	2028	Web Shear
	DC1-42-1.85-03	NSC	20.7	1067	533	533	267	2479	1.85	0.30	476	0.30	476	0.28	476	1886	Web Shear
	SS1-75-2.50-03	NSC	35.9	1067	533	635	267	3845	2.5	0.30	441	0.30	441	0.15	441	2887	Ledge (Punching Shear)
(Galal and Sekar 2008)	IT-G1	NSC	32	560	180	190	190	3600	2.24	1.09	440	0.19	440	0.19	440	230	Ledge (Hanger)
	IT-G2	NSC	31	560	180	190	190	3600	2.24	1.09	440	0.19	440	0.19	440	230	Ledge (Hanger)
	IT-G3	NSC	33	560	180	190	190	3600	2.24	1.09	440	0.57	440	0.57	440	254	Web Shear
	IT-G4	NSC	33.5	560	180	190	190	3600	2.24	1.09	440	0.57	440	0.57	440	258	Ledge (Punching Shear)
(Garber et al. 2017)	SS1-75-1.85-06	NSC	40.7	1067	533	635	267	3845	1.85	0.60	441	0.60	441	0.15	441	4062	Ledge (Punching Shear)
	SS1-75-2.5-06	NSC	44.1	1067	533	635	267	3845	2.5	0.60	441	0.60	441	0.15	441	4726	Ledge (Punching Shear)

Table 1 Continued

(Salman <i>et al.</i> 2019)	B1	NSC	29.8	300	100	80	100	2000	3.75	0.50	360	1.26	360	0.31	360	38	Flexural
	B2	NSC	32.2	300	100	80	100	2000	3.75	0.50	360	1.26	360	0.31	360	41	Flexural
	B3	NSC	32.2	300	100	80	100	2000	3.75	0.50	360	1.26	360	0.31	360	50	Flexural
	B4	NSC	32.2	300	100	80	100	2000	3.75	0.50	360	1.26	360	0.31	360	40	Flexural
	B5	NSC	32.2	300	100	80	100	2000	3.75	0.50	360	0.87	360	0.31	360	33	Flexural
	B6	NSC	32.2	300	100	80	100	2000	3.75	0.25	360	1.26	360	0.16	360	45	Web Shear
	B7	NSC	32.2	300	100	80	100	2000	3.75	0.50	360	1.26	360	0.31	360	50	Flexural
(Hedia <i>et al.</i> 2020)	BLN1	NSC	25.6	640	240	150	200	600	1.33	2.36	480	0.80	450	0.28	360	113	Ledge (Yield of ledge tie)
	BLN2	NSC	25.6	640	240	150	200	600	1.33	2.36	480	0.80	450	0.45	500	165	Ledge (Shear friction)
	BLN3	NSC	25.6	640	240	150	200	600	1.33	2.36	480	0.80	450	0.64	360	180	Ledge (Yield of ledge tie)
	BLN4	NSC	25.6	640	240	150	200	600	1.33	2.36	480	0.80	450	1.03	500	270	Ledge (Shear friction)
	BLH1	HSC	60	640	240	150	200	600	1.33	2.36	480	0.80	450	0.28	360	188	Ledge (Yield of ledge tie)
	BLH2	HSC	60	640	240	150	200	600	1.33	2.36	480	0.80	450	0.45	500	248	Ledge (Shear friction)
	BLH3	HSC	60	640	240	150	200	600	1.33	2.36	480	0.80	450	0.64	360	263	Ledge (Yield of ledge tie)
	BLH4	HSC	60	640	240	150	200	600	1.33	2.36	480	0.80	450	1.03	500	338	Ledge (Shear friction)
Average			34.7	867	407	360	230	3306	2.23	0.75	437	0.55	433	0.31	430.1	1671	
Minimum			20.7	300	100	80	100	600	1.33	0.25	360	0.19	360	0.15	360	33	-
Maximum			60	1067	533	635	267	6482	3.75	2.36	480	1.26	476	1.03	500	4726	

The collected experimental data passes through three stages:

- Training stage to predict the model.
- Validation stage to make sure that the algorithm is working as expected.
- Testing stage to explore the behavior of the developed models.

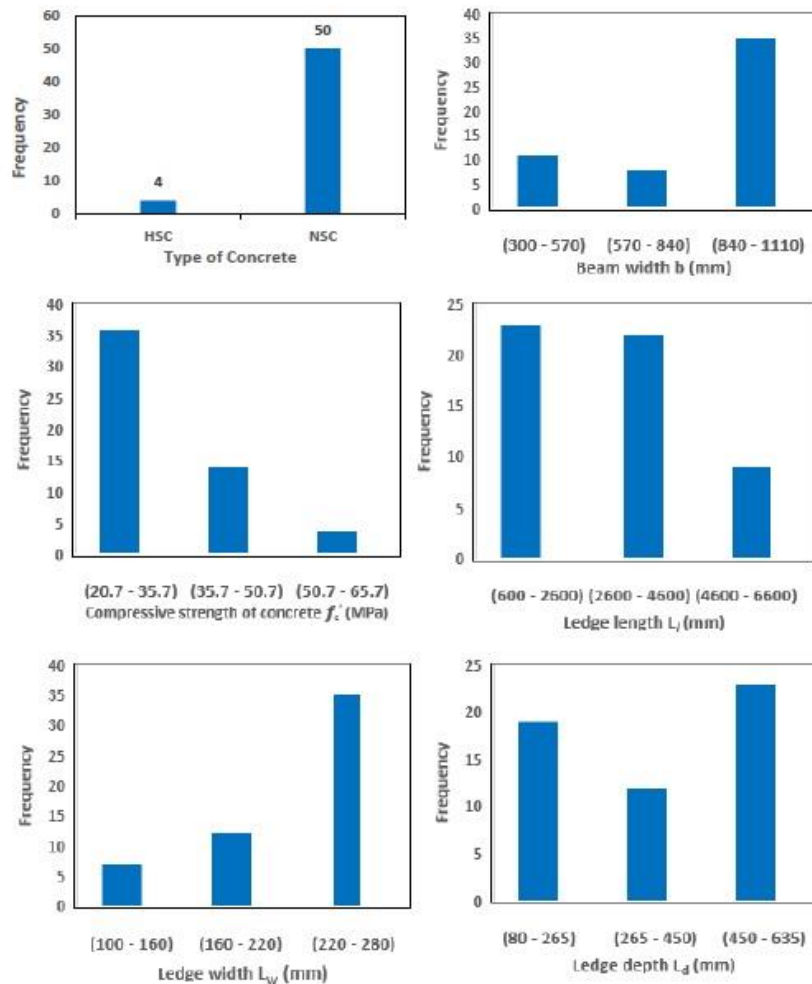
Decision Trees are a type of supervised ML used in MATLAB (that you explain what the input is and what the corresponding output is in the training data) where the data is continuously split in accord with a certain parameter. The tree can be explained by two entities, namely decision nodes and leaves. The leaves are the final outcomes, and the decision nodes are where the data is split (Rokach and Maimon 2005).

Support Vector Machine (SVM) is a supervised ML algorithm used in MATLAB that can be used for both classification or regression problems. However, it is usually used in classification problems. In the SVM algorithm, we plot each data item as a point in n-dimensional space (where n is the number of features you have) with the value of each feature being the value of a specific coordinate. Then, we perform classification by finding the hyper-plane that separates the two classes very well. Support vectors are simply the coordinates of individual observation. The SVM classifier is a frontier that best segregates the two classes (hyper-plane/ line) (Noble 2006).

K-Nearest Neighbor is one of the simplest ML algorithms used in MATLAB and based on supervised learning technique. It considers the similarity between the new case and available cases and put the new case into the category that is most related to the available categories. K-NN algorithm stores all the available data and classifies a new data point based on the similarity. This means when new data appears then it can be simply classified into a well suite category by using K-NN algorithm as shown in Fig. 5. It can be used for regression as well as for classification, but it is usually used for the classification problems. K-NN is a non-parametric algorithm, which means it does not make any assumption on underlying data (Keller *et al.* 1985).

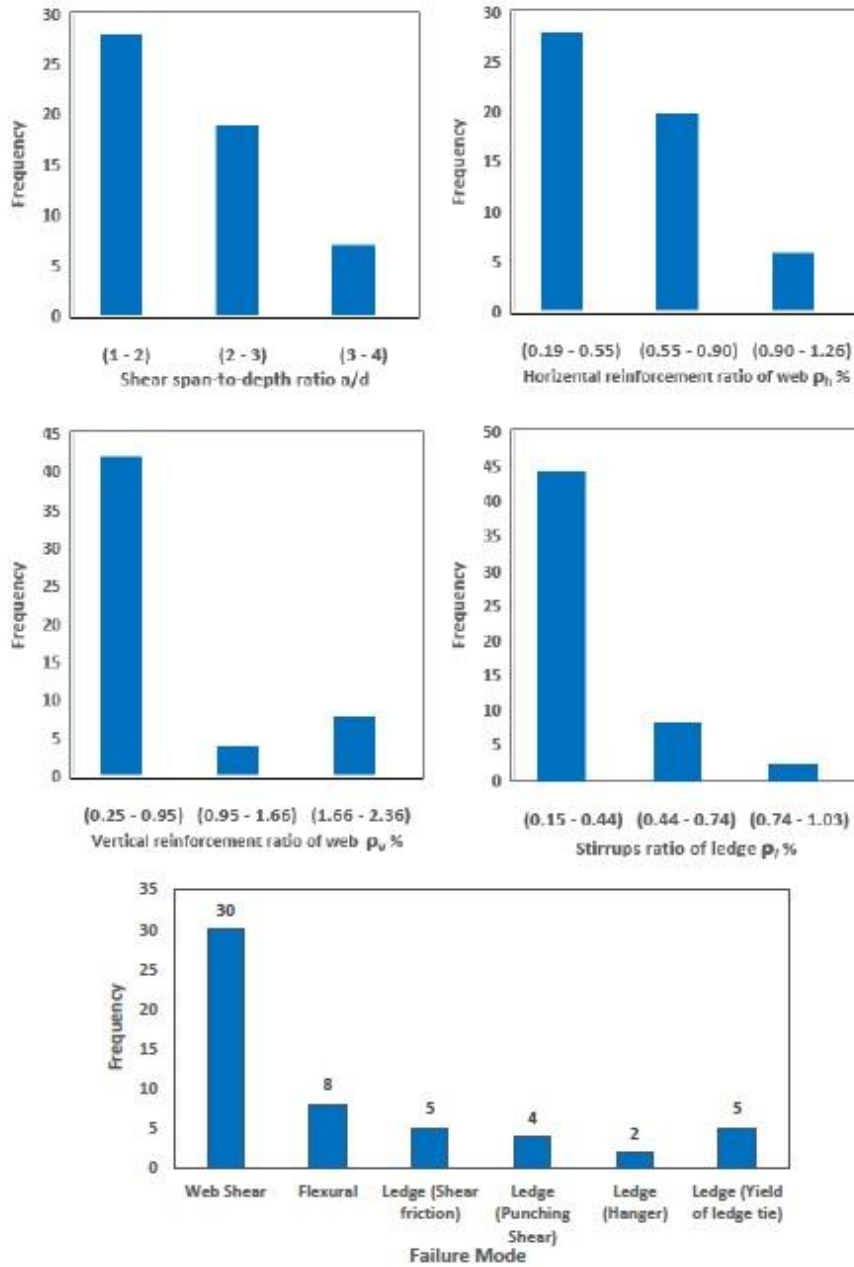
Naive Bayes algorithm is a classification technique used in MATLAB and based on Bayes' Theorem with an assumption of independence among predictors. In simple terms, a Naive Bayes classifier assumes that the presence of a particular feature in a class is unrelated to the presence of any other feature. Naive Bayes model is easy to build and particularly useful for very large data sets. Along with simplicity, Naive Bayes is known to outperform even highly sophisticated classification methods (Berrar 2018).

Linear discriminant analysis in ML used in MATLAB means that each class (Y) generates data (X) using a multivariate normal distribution. In other words, the model considers (X) has a Gaussian mixture distribution. For linear discriminant analysis, the model has the same covariance matrix for each class; only the means differ (Balakrishnama and Ganapathiraju 1998). It computes the sample mean of each class. Then it computes the sample covariance by first subtracting the sample mean of each class from the observations of that class and taking the empirical covariance matrix of the result.



(a)

Fig. 3 (a) Distribution of different variables in the experimental dataset and (b) Distribution of different variables in the experimental dataset



(b)

Fig. 3 Continued-

Prediction by linear discriminant analysis uses three quantities to classify observations including posterior probability, prior probability, and cost. Prediction is classified to minimize the expected classification cost.

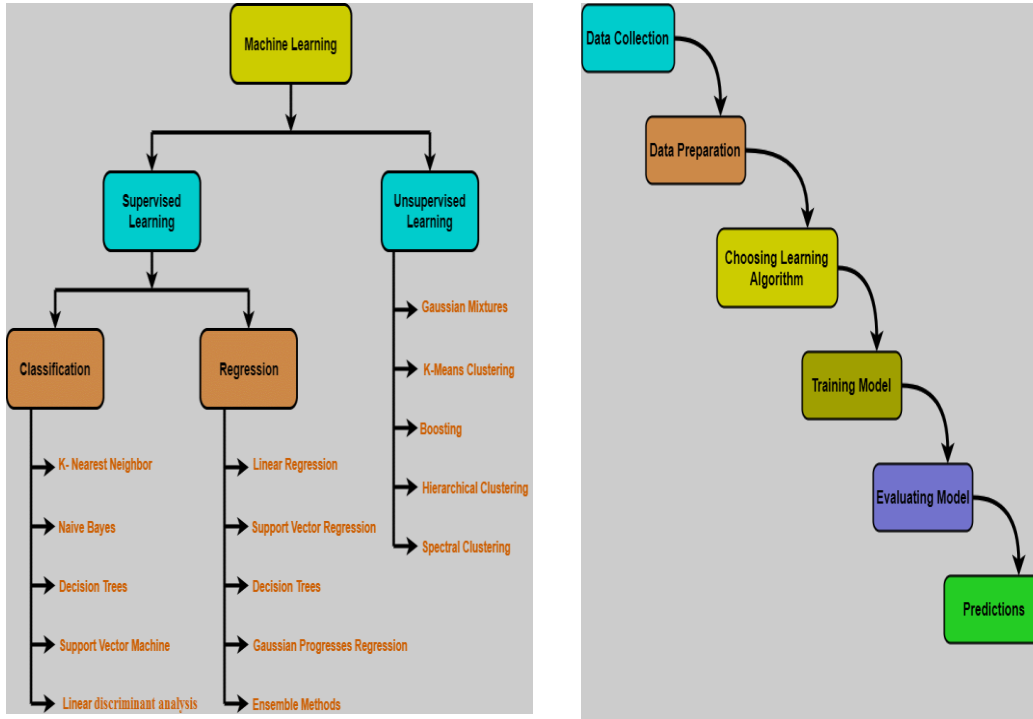


Fig. 4 Process of Machine learning framework

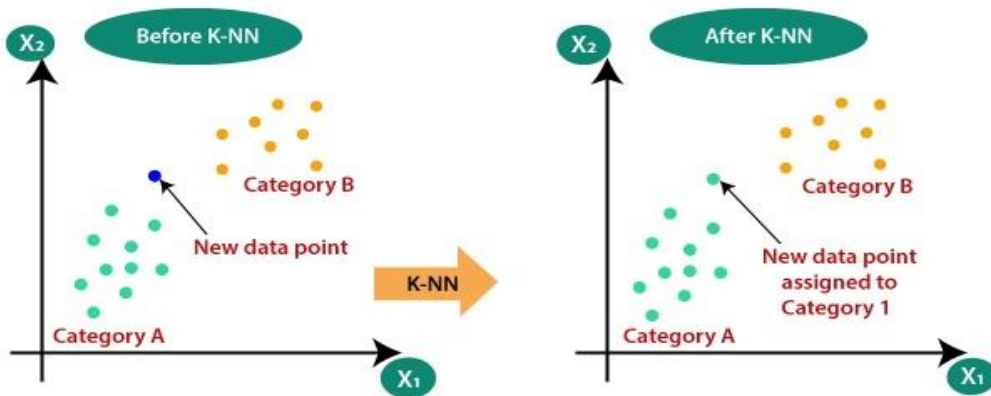


Fig. 5 K-Nearest Neighbor

Ensemble methods are learning algorithms that create a set of classifiers and then classify new data points by taking a weighted vote of their predictions. The original ensemble method is Bayesian averaging, but more new algorithms include error-correcting output coding, bagging, and boosting (Dietterich 2000).

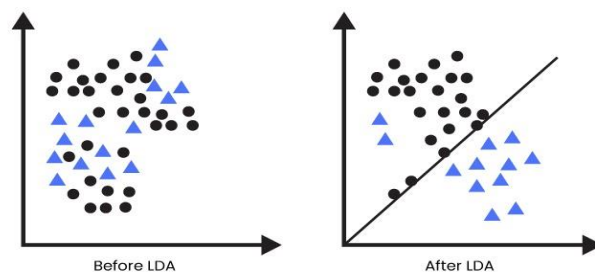


Fig. 6 Linear discriminant analysis

#### 4.2 Linear discriminant analysis

The best overall accuracy from all models based on linear discriminant analysis was 86% as linear discriminant analysis can separate two or more classes of objects with best performance as shown in Fig. 6. The flowchart for the linear discriminant analysis is shown in Fig. 7. In order to check the quality of classification The receiver operating characteristic (ROC) was plotted in Figs. 8-10. The area under ROC curve (AUC) being 1 indicates the best performance. So, an AUC value close to unity means better failure mode classification. AUC values for web shear, flexural and ledge failure mode were 0.81, 0.85 and 0.85.

In order to examine the behavior of ML algorithms, a confusion matrix containing information on actual and predicted classifications was employed and plotted on the studied test dataset. It displays the total number of observations in each cell. The rows of the confusion matrix refer to the true class, and the columns refer to the predicted class. Diagonal and off-diagonal cells refer to correctly and incorrectly classified observations. For a particular class ( $i$ ), the True Positive Ratio (TPR) is the number of outputs whose actual and predicted class is class  $i$ , divided by the number of outputs whose predicted class is class  $i$ , and the False Positive Ratio (FPR) is the number of outputs whose actual class is not class  $i$ , but predicted class is class  $i$ , divided by the number of outputs whose predicted class is not class  $i$ . The Positive Predictive Values (PPV) is the proportion of correctly classified observations per predicted class. False Discovery Rates (FDR) is the proportion of incorrectly classified observations per predicted class (Moore and Sanadhya 2007).

The column on the far right of the plot shows the percentages of all the examples predicted belonging to each class that are correctly and incorrectly classified. These metrics are usually called the precision (or positive predictive value) and false discovery rate, respectively. The row at the bottom of the plot shows the percentages of all the examples belonging to each class that are correctly and incorrectly classified. These metrics are usually called the recall (or true positive rate) and false negative rate, respectively.

A confusion matrix represents the actual failure modes versus the predicted failure mode was applied on the studied test dataset as shown in Fig. 11. As explained before, there are 3 classes of failure modes related to reinforced concrete ledge beams either web shear, flexural or ledge failure. According to the confusion matrix as shown in Fig. 11, the precision and recall for ledge failure mode were 75% and 92.3%, the precision and recall for the web shear failure mode were 93.3% and 82.4% and the precision and recall for flexural failure mode were 75% and 85.7%. These results show that the proposed ML algorithms can effectively predict the failure mode classification of reinforced concrete ledge beams.

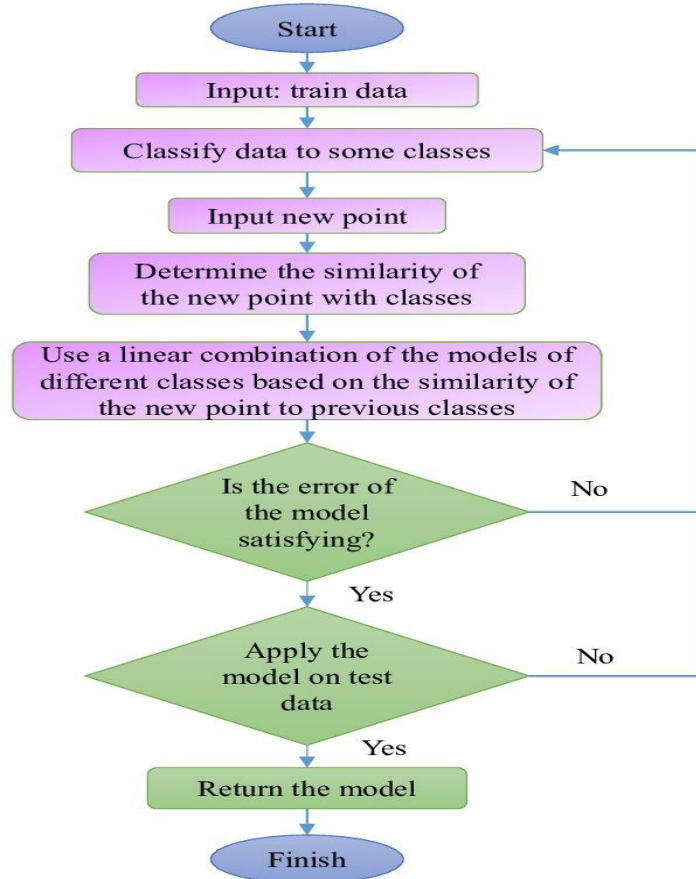


Fig. 7 A flowchart for the linear discriminant analysis

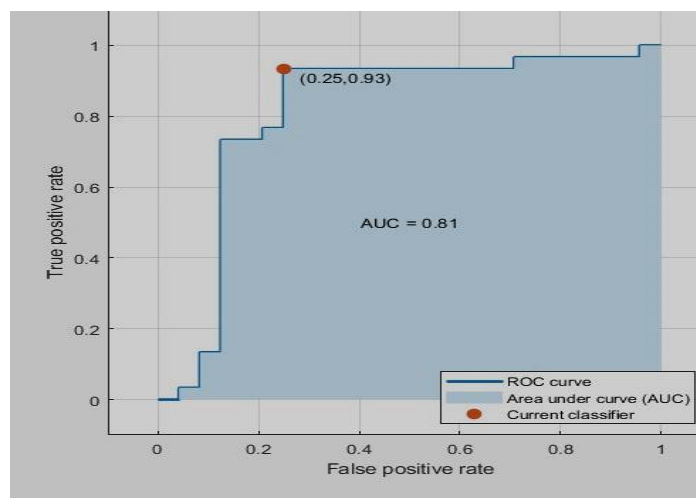


Fig. 8 ROC curve for web shear failure mode classification (AUC = 0.81)

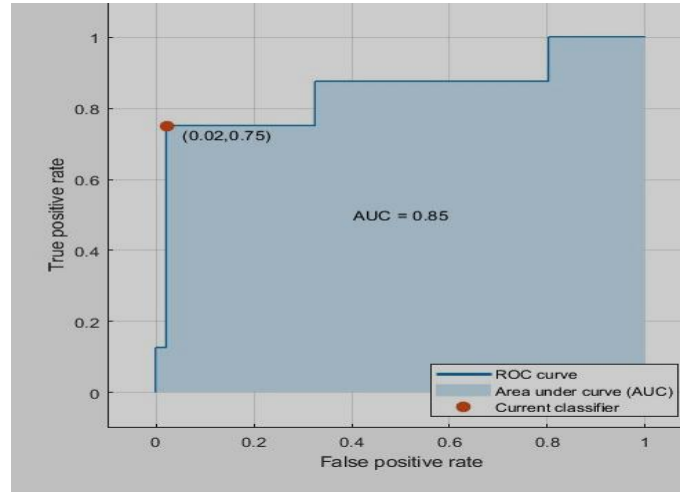


Fig. 9 ROC curve for flexural failure mode classification (AUC = 0.85)

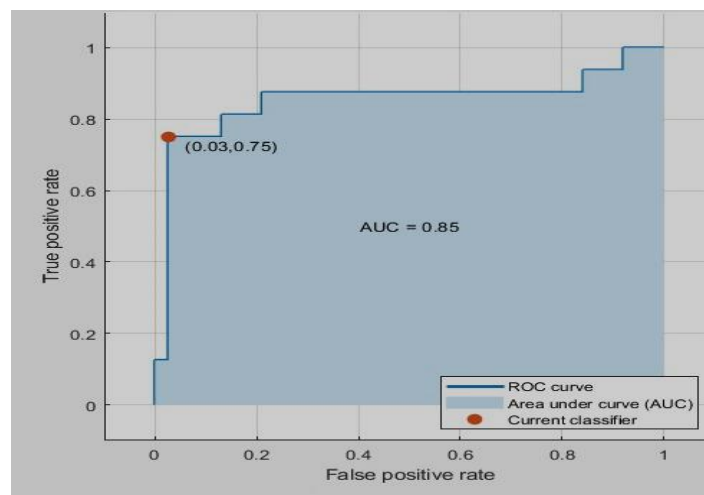
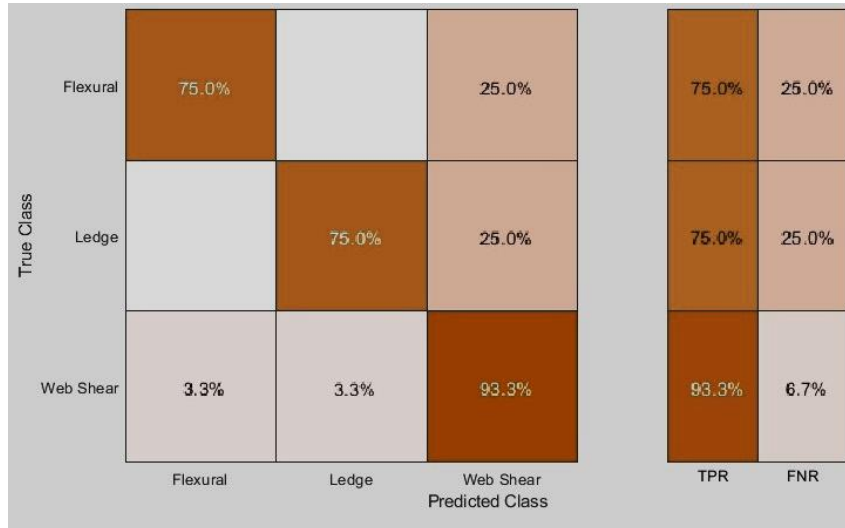


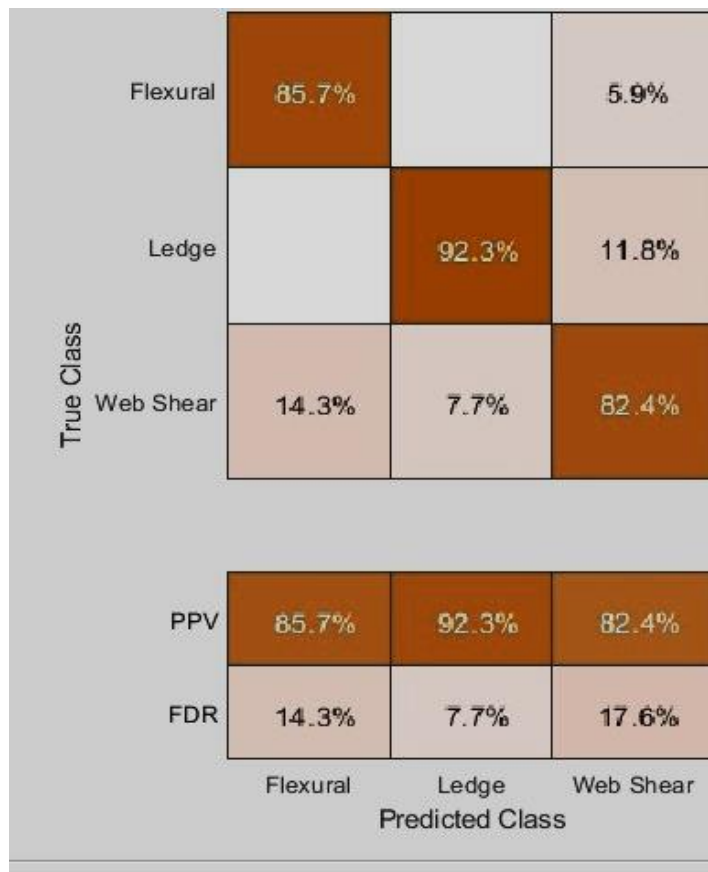
Fig. 10 ROC curve for ledge failure mode classification (AUC = 0.85)

## 5. ML framework for prediction of ultimate shear strength

The main variables for prediction the ultimate shear strength includes  $f'_c$ ,  $d$ ,  $b$ ,  $b_w$ ,  $L_d$ ,  $L_w$ ,  $L_l$ ,  $a/d$ ,  $\rho_v$ ,  $f_{yv}$ ,  $\rho_h$ ,  $f_{yh}$ ,  $\rho_l$ ,  $f_{yl}$  and  $V_u$ . Multiple linear regression analysis was used to develop equations to predict the ultimate shear strength of RC ledge beams based on the type of the failure. Regression models are used to describe relationships between variables by fitting a line to the observed data. Regression allows you to estimate how a dependent variable changes as the independent variable(s) change. Multiple linear regression is used to estimate the relationship between two or more independent variables and one dependent variable as shown in Fig. 12. The equation of multiple linear regression is defined as



(a)



(b)

Fig. 11 (a) Confusion matrix (TPR and FNR) for failure mode classification (b) Confusion matrix (PPV and FDR) for failure mode classification

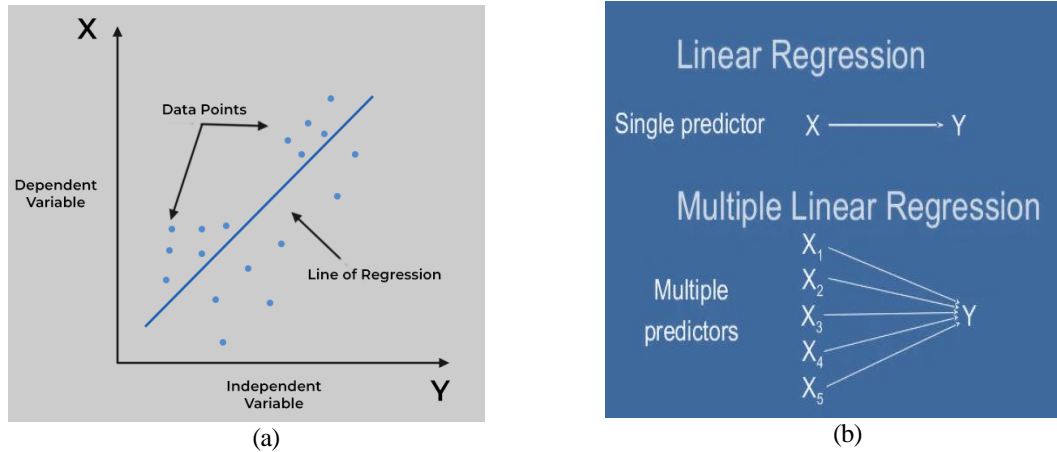


Fig. 12 (a) Concept of linear regression and (b) Difference between linear and multiple linear regression

$$Y = a + b_1X_1 + b_2X_2 + \dots + b_nX_n + \varepsilon \quad (1)$$

Where

Y : Dependent variable of the regression

$X_n$  : Independent variable of the regression

a : y-intercept (constant term)

$b_n$  : Slope of the regression

$\varepsilon$  : The error term

The derived equations of each failure mode either web shear, flexural or ledge failure are shown in Table 2 based on the studied critical parameters. The coefficient of determination ( $R^2$ ) is also shown in Table 2. It should be noted that the best equation is the one that has  $R^2$  value close to 100%.

The coefficient of determination ( $R^2$ ) can be determined as

$$R^2 = 1 - \frac{\text{sum squared regression (SSR)}}{\text{total sum of squares (SST)}} = 1 - \frac{\sum (y_i - \hat{y}_i)^2}{\sum (y_i - \bar{y})^2} \quad (2)$$

Where

$y_i$  : The y value for observation i

$\bar{y}$  : The mean of y value

$\hat{y}_i$  : The predicted value of y for observation i

## 6. Comparison study for reinforced concrete ledge beams

In order to show the reliability of the derived expressions, a comparison of the ultimate shear strength for different ledge failure modes was conducted between results obtained from the proposed ML models and the results from the reported experiments. In addition, the accuracy of the equations used by AASHTO LRFD-2020 and PCI-2020 for evaluating the shear strength of reinforced concrete ledge beams was examined.

Table 2 Derived equations for prediction of ultimate shear strength of reinforced concrete ledge beams

Type of failure	Derived Equation	R <sup>2</sup> (%)
Web Shear failure	$V_u = \sqrt{f'_c} b_w d (0.233 a/d + 0.161 \rho_v f_{yv} - 0.0247 \rho_h f_{yh})$	89.2%
Flexural failure	$V_u = \sqrt{f'_c} b_w d (-0.234 a/d - 0.167 \rho_v f_{yv} + 0.087 \rho_h f_{yh} + 1.442 \rho_l f_{yl})$	98.3%
Ledge failure	$V_u = 5.49 f'_c + 7.86 L_d + 2.43 L_w - 0.07 L_l + 36.35 \rho_l f_{yl} - 1736.43$	94.6%
General failure	$V_u = \sqrt{f'_c} b_w d (0.0003 L_d + 0.002 L_w + 0.00005 L_l - 0.1 a/d - 0.05 \rho_v f_{yv} + 0.12 \rho_h f_{yh} + 0.06 \rho_l f_{yl})$	96.1%

$\rho_v$ ,  $\rho_h$  and  $\rho_l$  are in percentage.  
Stresses are in MPa and dimensions are in mm.

Table 3 Design equations used by AASHTO LRFD-2020 for calculating the shear strength of reinforced concrete ledge beams

Type of failure	Equation
	$V_u = \phi c A_{cv} + \mu \phi (A_{vf} F_y + P_c)$
Shear friction failure between the ledge and the web	$V_u \leq \phi K_1 f'_c A_{cv}$
	$V_u \leq \phi K_2 A_{cv}$
	$V_u \leq (3.3 + 0.08 * f'_c) \phi A_{cv}$
Punching shear failure at load point	$V_u = 0.125 \sqrt{f'_c} (W + 2L + 2d_e) \phi d_e$ (c is greater than S/2)
	$V_u = 0.125 \sqrt{f'_c} (W + L + d_e) \phi d_e$ (close to the edge)
	$V_u = 0.125 \sqrt{f'_c} (0.5W + L + d_e + c) \phi d_e$ (others)
Failure of hanger reinforcement	$V_u = \frac{A_{hr}(0.5f_y)}{s} (W + 3a_f) \phi$ (service limit state)
	$V_u = \frac{A_{hr} f_y}{s} S \phi$ (strength limit state)
	$V_u = 0.165 \sqrt{f'_c} b_f \phi d_f + \frac{A_{hr} f_y}{s} \phi (W + 2d_f)$ (strength limit state)
Flexural failure of ledge reinforcement	$A_s \geq \frac{2A_{vf}}{3} + A_n$ <span style="float: right;"><math>A_n \geq \frac{N_{uc}}{\phi f_y}</math></span>
Bearing of concrete under the load point	$P_u = 0.85 f'_c A_1 m \phi$

### 6.1 AASHTO LRFD-2020

The shear capacity of each failure of ledge either shear friction, punching shear, hanger reinforcement, flexural or bearing are shown in Table 3 according to the design equations of AASHTO.

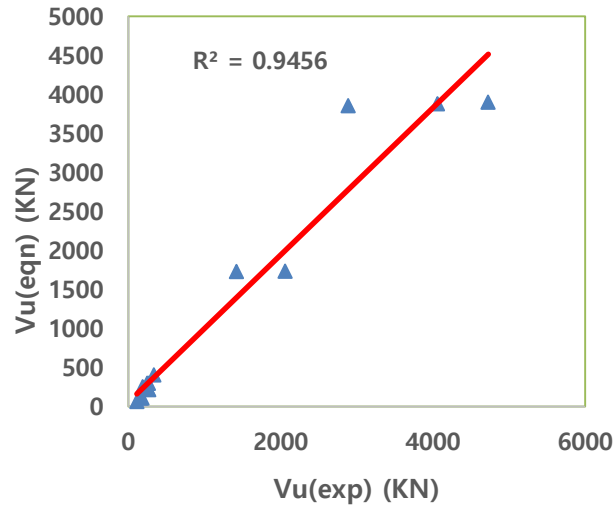


Fig. 13 Comparison study with the derived equations ( $R^2 = 94.6\%$ )

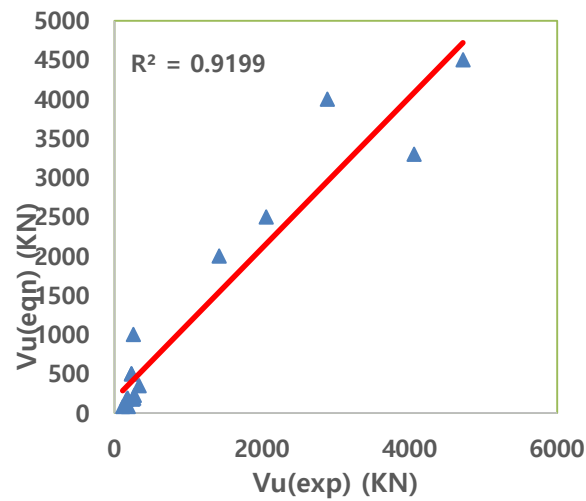


Fig. 14 Comparison study with the design equations of AASHTO LRFD-2020 ( $R^2 = 91.9\%$ ).

A graphical comparison of ultimate shear strength of ledge failure of reinforced concrete ledge beams between results from experimental data and derived equation is shown in Fig. 13, while comparison between collected test data and equations from AASHTO appears in Fig. 14. It can be clearly observed that the proposed equations where  $R^2$  is 94.6% showed better performance than the design equations of AASHTO LRFD-2020 where  $R^2$  is 91.9%.

## 6.2 PCI-2020

The equations of shear strength of ledge, transverse bending of ledge, longitudinal bending of

Table 4 Design equations used by PCI-2020 for calculating the shear strength of reinforced concrete ledge beams

Type	Equation
Shear strength of ledge	For $s > b_t + h_l$
	$V_u = 3\phi\lambda\sqrt{f'_c} h_l [2(b_l - b) + b_t + h_l]$
	$V_u = \phi\lambda\sqrt{f'_c} h_l [2(b_l - b) + b_t + h_l + 2de]$
	For $s < b_t + h_l$
Shear strength of ledge	$V_u = 1.5\phi\lambda\sqrt{f'_c} h_l [2(b_l - b) + b_t + h_l + s]$
	$V_u = \phi\lambda\sqrt{f'_c} h_l [(b_l - b) + (\frac{b_t + h_l}{2}) + de + s]$
Transverse (cantilever) bending of ledge	$A_s = \frac{1}{\phi f_y} [V_u (\frac{a}{d}) + N_u (\frac{h_l}{d})]$
Longitudinal bending of ledge	$A_l = 200(b_l - b) d_l / f_y$
Attachment of ledge to web	$A_s = \frac{V_u}{\phi f_y} (m)$
Out-of-plane bending near beam end	$A_{wv} = A_{wl} = \frac{V_u e}{2\phi f_y d_w}$

//

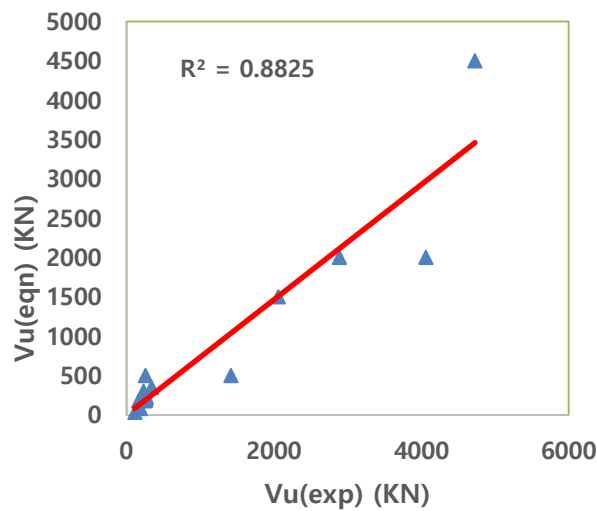


Fig. 15 Comparison study with the design equations of PCI-2020 ( $R^2 = 88.2\%$ )

ledge, attachment of ledge to web and out-of-plane bending near beam end is shown in Table 4 according to PCI-2020.

A graphical comparison of ultimate shear strength of ledge of reinforced concrete ledge beams between collected test data and equations from PCI appears in Fig. 15. It can be clearly observed that the proposed equation where  $R^2$  is 94.6% showed better performance than the design equations of PCI-2020 where  $R^2$  is 88%

## 7. Limitations

- All the available experimental data were collected in the database, but by increasing the number of specimens the performance of the machine learning framework can be improved.
- The derived equations are valid for the range of critical variables ( $f'_c$ ,  $d$ ,  $b$ ,  $b_w$ ,  $L_d$ ,  $L_w$ ,  $L_l$ ,  $a/d$ ,  $\rho_v$ ,  $f_{yv}$ ,  $\rho_h$ ,  $f_{yh}$ ,  $\rho_l$ ,  $f_{yl}$ ) as shown in Table 1.

## 8. Conclusions

A data-driven machine learning (ML) framework for predicting ultimate shear strength and failure modes of reinforced concrete ledge beams has been presented. The available database was analyzed using different ML algorithms to identify critical parameters of reinforced concrete ledge beams. Based on the results of this study, the following can be concluded:

- The critical parameters governing prediction of ultimate shear strength and failure mode of reinforced concrete ledge beams are design compressive strength of concrete, beam depth, beam width, beam web width, ledge depth, ledge width, ledge length, shear span-to-depth ratio, web vertical reinforcement ratio, yield strength of web vertical reinforcement, web horizontal reinforcement ratio, yield strength of web horizontal reinforcement, vertical reinforcement ratio of ledge and yield strength of vertical reinforcement of ledge.
- Machine learning algorithms can effectively predict different failure modes of reinforced concrete ledge beams either web shear failure, flexural failure, or ledge failure. The best ML algorithm is linear discriminant analysis with an overall accuracy of 86%.
- The proposed ML equations showed good predictions for ultimate shear strength of different failure modes of reinforced concrete ledge beams and can be safely used for design purposes.
- The predictions of ultimate shear strength of ledge of reinforced concrete ledge beams using the proposed ML equations indicated better performance than the design equations of AASHTO LRFD-2020 or PCI-2020.

## References

- AASHTO LRFD (2020), Bridge Design Specifications 9th edition, American Association of State Highway and Transportation Officials, Washington, D.C.
- Abuodeh, O.R., Abdalla, J.A. and Hawileh, R.A. (2020), "Prediction of shear strength and behavior of RC beams strengthened with externally bonded FRP sheets using machine learning techniques", *Compos. Struct.*, **234**, 111698. <https://doi.org/10.1016/j.compstruct.2019.111698>.
- ACI Committee 318 (2019), 'Building Code Requirements for Structural Concrete (ACI 318-19) and Commentary (ACI 318R-19)', American Concrete Institute. Farmington Hills, Michigan 48333-9094.
- Balakrishnama, S. and Ganapathiraju, A. (1998), "Linear discriminant analysis-a brief tutorial", *Institute for Signal and information Processing*, **18**, 1-8.
- Bayrak, O., Larson, N., Gomez, E.F. (2013), "Shear Cracking in Inverted-T Straddle Bents", Research Report No. 0-6416, The University of Texas, Texas.
- Berrar, D. (2018), "Bayes' theorem and naive bayes classifier", *Encyclopedia of Bioinformatics and Computational Biology: ABC of Bioinformatics*, Elsevier Science Publisher, Amsterdam, The Netherlands, 403-412.
- Bircher, D., Tuchscherer, R., Huizinga, M., Bayrak, O., Wood, S.L. and Jirsa, J.O. (2009), "Strength and

- serviceability design of reinforced concrete deep beams”, No. FHWA/TX-09/0-5253-1.
- Chalioris, C.E. and Karayannis, C.G. (2009), “Effectiveness of the use of steel fibres on the torsional behaviour of flanged concrete beams”, *Cement Concrete Compos.*, **31**(5), 331-341. <https://doi.org/10.1016/j.cemconcomp.2009.02.007>.
- Cheung, A., Cabrera, C., Sarabandi, P., Nair, K.K., Kiremidjian, A. and Wenzel, H. (2008), “The application of statistical pattern recognition methods for damage detection to field data”, *Smart Mater. Struct.*, **17**(6), 065023. <https://doi.org/10.1088/0964-1726/17/6/065023>.
- Chou, J.S., Tsai, C.F., Pham, A.D. and Lu, Y.H. (2014), “Machine learning in concrete strength simulations: Multi-nation data analytics”, *Constr. Build. Mater.*, **73**, 771-780. <https://doi.org/10.1016/j.conbuildmat.2014.09.054>.
- Dantas, A.T.A., Leite, M.B. and de Jesus Nagahama, K. (2013), “Prediction of compressive strength of concrete containing construction and demolition waste using artificial neural networks”, *Constr. Build. Mater.*, **38**, 717-722. <https://doi.org/10.1016/j.conbuildmat.2012.09.026>.
- Deifalla, A. and A. Ghobarah (2014), “Behavior and analysis of inverted T-shaped RC beams under shear and torsion”, *Eng. Struct.*, **68**, 57-70. <https://doi.org/10.1016/j.engstruct.2014.02.011>.
- Deifalla, A. and Ghobarah, A. (2006), “Assessing the north american bridge codes for the design of T-girders under torsion and shear”. *Proceeding of the 7th international conference on short & medium span bridges*, Montreal.
- Deifalla, A. and Ghobarah, A. (2006), “Calculating the thickness of FRP jacket for shear and torsion strengthening of RC T-Girders”. in third international conference on FRP composites in civil engineering (CICE), Miami, FL.
- Dietterich, T.G. (2000), “Ensemble methods in machine learning”, International workshop on multiple classifier systems, Springer.
- Fereig, S. and Smith, K. (1977), “Indirect loading on beams with short shear spans”, *Journal Proceedings*.
- Fernandez Gomez, E. (2012), “Design criteria for strength and serviceability of inverted-T straddle bent caps”, PhD dissertation, The University of Texas, Texas.
- Furlong, R. and Mirza, S. (1974), Strength and serviceability of inverted-T beam caps subjected to combined flexure, shear and torsion.
- Furlong, R.W., Ferguson, P.M. and Ma, J.S. (1971), “Shear and anchorage study of reinforcement in inverted T-beam bent cap girders”, Center for highway research, University of Texas at Austin, **113**.
- Galal, K. and Sekar, M. (2008), “Rehabilitation of RC inverted-T girders using anchored CFRP sheets”, *Compos. Part B: Eng.*, **39**(4), 604-617. <https://doi.org/10.1016/j.compositesb.2007.09.001>.
- Garber, D.B. (2011), “Shear cracking in inverted-T straddle bents”, PhD dissertation, The University of Texas, Texas.
- Garber, D.B., Varney, N.L., Gómez, E.F. and Bayrak, O. (2017), “Performance of ledges in inverted-T beams”, *ACI Struct. J.*, **114**(2), 487-498. <https://doi.org/10.14359/51689451>.
- González, M.P. and Zapico, J.L. (2008), “Seismic damage identification in buildings using neural networks and modal data”, *Comput. Struct.*, **86**(3-5), 416-426. <https://doi.org/10.1016/j.compstruc.2007.02.021>.
- Gui, G., Pan, H., Lin, Z., Li, Y. and Yuan, Z. (2017), “Data-driven support vector machine with optimization techniques for structural health monitoring and damage detection”, *KSCE J. Civil Eng.*, **21**(2), 523-534. <https://doi.org/10.1007/s12205-017-1518-5>.
- Gul, M. and Catbas, F.N. (2009), “Statistical pattern recognition for structural health monitoring using time series modeling: theory and experimental verifications”, *Mech. Syst. Signal Pr.*, **23**(7), 2192-2204. <https://doi.org/10.1016/j.ymsp.2009.02.013>.
- He, L., Guo, H., Jin, Y., Zhuang, X., Rabczuk, T. and Li, Y. (2022), “Machine-learning-driven on-demand design of phononic beams”, *Science China Physics, Mechanics & Astronomy*, **65**(1), 1-12.
- Hedia, M.H., El-Metwally, S.E. and Yousef, A.M. (2020), “Behavior of Ledges in Inverted-T Beams”, Ms.c. Dissertation, Mansoura University, Mansoura.
- Hedia, M.H., El-Metwally, S.E. and Yousef, A.M. (2020), “Design of reinforced concrete ledge beams safety and economy”, *Eng. Res. J.*, **166**, 242-261.
- Karayannis, C. (1995), “Torsional analysis of flanged concrete elements with tension softening”, *Comput.*

- Struct.*, **54**(1), 97-110. [https://doi.org/10.1016/0045-7949\(94\)00299-I](https://doi.org/10.1016/0045-7949(94)00299-I).
- Karayannis, C.G. and Chalioris, C.E. (2000), "Experimental validation of smeared analysis for plain concrete in torsion", *J. Struct. Eng.*, **126**(6), 646-653. [https://doi.org/10.1061/\(ASCE\)0733-9445\(2000\)126:6\(646\)](https://doi.org/10.1061/(ASCE)0733-9445(2000)126:6(646)).
- Keller, J.M., Gray, M.R. and Givens, J.A. (1985), "A fuzzy k-nearest neighbor algorithm", *IEEE T. Syst. Man Cy.*, **4**, 580-585. <https://doi.org/10.1109/TSMC.1985.6313426>.
- Klein, G.J. (1986), "Design of spandrel beams", *PCI J.*, **31**, 76-124. <https://doi.org/10.15554/pcij.09011986.76.124>.
- Larson, N., Gomez, E.F., Garber, D., Bayrak, O. and Ghannoum, W. (2013), "Strength and serviceability design of reinforced concrete inverted-T beams", Research Report No. FHWA/TX-13/0-6416-1. 2013, The University of Texas, Texas.
- Ly, H.B., Le, T.T., Vu, H.L.T., Tran, V.Q., Le, L.M. and Pham, B.T. (2020), "Computational hybrid machine learning based prediction of shear capacity for steel fiber reinforced concrete beams", *Sustainability*, **12**(7), 2709. <https://doi.org/10.3390/su12072709>.
- Markou, G. and Bakas, N.P. (2021), "Prediction of the shear capacity of reinforced concrete slender beams without stirrups by applying artificial intelligence algorithms in a big database of beams generated by 3d nonlinear finite element analysis", *Comput. Concrete*, **28**(6), 533-547. <https://doi.org/10.12989/cac.2021.28.6.533>.
- Mirza, S. and Furlong, R. (1985), "Design of reinforced and prestressed concrete inverted T beams for bridge structures", *PCI J.*, **30**(4), 112-137.
- Mirza, S., Furlong, R. and Ma, J. (1989), "Flexural shear and ledge reinforcement in reinforced concrete inverted T-girders", *Struct. J.*, **85**(5), 509-520. <https://doi.org/10.14359/2790>.
- Mirza, S.A. and Furlong, R.W. (1983), "Serviceability behavior and failure mechanisms of concrete inverted T-beam bridge bent caps", *J. Proceedings*, **80**(4), 294-304. <https://doi.org/10.14359/10850>.
- Mirza, S.A. and Furlong, R.W. (1983), "Strength criteria for concrete inverted T girders", *Struct. Eng.*, **109**(8), 1836-1853. <https://doi.org/10.1016/j.engstruct.2014.02.011>.
- Noble, W.S. (2006), "What is a support vector machine?", *Nature Biotechnol.*, **24**(12), 1565-1567. <https://doi.org/10.1038/nbt1206-1565>.
- PCI Design Handbook (2020), 8th edition Precast and Prestressed Concrete. Chicago: Precast/Prestressed Concrete Institute.
- Rahman, J., Ahmed, K.S., Khan, N.I., Islam, K. and Mangalathu, S., (2021), "Data-driven shear strength prediction of steel fiber reinforced concrete beams using machine learning approach", *Eng. Struct.*, **233**, 111743. <https://doi.org/10.1016/j.engstruct.2020.111743>.
- Reddy, T.A., Devi, K.R. and Gangashetty, S.V. (2011), "Multilayer feedforward neural network models for pattern recognition tasks in earthquake engineering", *Proceedings of the International Conference on Advanced Computing, Networking and Security*, Springer, Berlin, Heidelberg.
- Rokach, L. and Maimon, O. (2005), "Decision trees. Data mining and knowledge discovery handbook", Springer.
- Salehi, H., Das, S., Chakrabarty, S., Biswas, S. and Burgueño, R. (2018), "Structural damage identification using image-based pattern recognition on event-based binary data generated from self-powered sensor networks", *Struct. Control Health Monit.*, **25**(4), e2135. <https://doi.org/10.1002/stc.2135>.
- Salehi, H., Das, S., Chakrabarty, S., Biswas, S. and Burgueño, R. (2019), "An algorithmic framework for reconstruction of time-delayed and incomplete binary signals from an energy-lean structural health monitoring system", *Eng. Struct.*, **180**, 603-620. <https://doi.org/10.1016/j.engstruct.2018.11.072>.
- Salman, W.A., El-kersh, I.H., Lotfy, E.M. and Ahmed, M.A. (2019), "Behavior of reinforced concrete inverted T-section beams containing Nano-silica", *IOSR J. Mech. Civil Eng. (IOSR-JMCE)*, **16**(5), 13-22.
- Siddique, R., Aggarwal, P. and Aggarwal, Y. (2011), "Prediction of compressive strength of self-compacting concrete containing bottom ash using artificial neural networks", *Adv. Eng. Software*, **42**(10), 780-786. <https://doi.org/10.1016/j.advengsoft.2011.05.016>.
- Smith, K. and Fereig, S. (1974), "Effect of loading and supporting conditions on the shear strength of deep beams", *Special Publication*, **42**, 441-460.
- Solhmirzaei, R., Salehi, H., Kodur, V. and Naser, M.Z. (2020), "Machine learning framework for predicting

- failure mode and shear capacity of ultra high performance concrete beams”, *Eng. Struct.*, **224**, 111221. <https://doi.org/10.1016/j.engstruct.2020.111221>.
- Tan, K., Kong, F. and Weng, L. (1997), “High strength concrete deep beams subjected to combined top-and bottom-loading”, *Struct. Engineer*, **75**(11).
- Uddin, M.N., Yu, K., Li, L., Ye, J., Tafsirojjaman, T. and Alhaddad, W. (2022), “Developing machine learning model to estimate the shear capacity for RC beams with stirrups using standard building codes”, *Innov. Infrastructure Solutions*, **7**(3), 1-20. <https://doi.org/10.1007/s41062-022-00826-8>.
- Varney, N.L., Fernandez-Gomez, E., Garber, D.B., Ghannoum, W.M. and Bayrak, O. (2015), “Inverted-T Beams: experiments and strut-and-tie modeling”, *ACI Struct. J.*, **112**(2), 147-156.
- Wakjira, T.G., Al-Hamrani, A., Ebead, U. and Alnahhal, W. (2022), “Shear capacity prediction of FRP-RC beams using single and ensemble Explainable Machine learning models”, *Compos. Struct.*, **287**, 115381. <https://doi.org/10.1016/j.compstruct.2022.115381>.
- Yan, K. and Shi, C. (2010), “Prediction of elastic modulus of normal and high strength concrete by support vector machine”, *Constr. Build. Mater.*, **24**(8), 1479-1485. <https://doi.org/10.1016/j.conbuildmat.2010.01.006>.
- Yang, W.Y., Cao, W., Kim, J., Park, K.W., Park, H.H., Joung, J., Ro, J.S., Lee, H.L., Hong, C.H. and Im, T. (2020), “Applied numerical methods using MATLAB”, John Wiley & Sons, Hoboken, New Jersey, USA.
- Zhang, J., Sun, Y., Li, G., Wang, Y., Sun, J. and Li, J. (2020), “Machine-learning-assisted shear strength prediction of reinforced concrete beams with and without stirrups”, *Eng. with Comput.*, 1-15. <https://doi.org/10.1007/s00366-020-01076-x>.
- Zhu, R.H., Dhonde, H. and Hsu, T.T.C. (2003), “Crack control for ledges in inverted-T bent caps”, Research Report No 0-1854-5m University of Houston, Department of Civil & Environmental Engineering.